Metallurgical and Materials Engineering *Research paper*
Association of Metallurgical Engineers of Serbia AMES *https://doi.org/10.30544/816*

INVESTIGATION ON CORROSION AND WEAR PROPERTIES OF Al-7075/TiC COMPOSITES FABRICATED BY STIR CASTING ROUTE

Manoj Velishala, Mahesh Pandiripalli, C.Vanitha [*]

Department of Metallurgical and Materials Engineering, National Institute of Technology Warangal, Telangana state, India

Received 29.03.2022

Accepted 03.07.2022

Abstract

Metal matrix composites (MMCs) play a crucial role in the aerospace, automotive and mineral processing industries. The properties of aluminum matrix composites (AMC) that are renowned for their high strength, good stiffness and excellent thermal conductivity can be enhanced by incorporating various reinforcements. In this investigation, Al7075 alloy with TiC (3, 6, and 9 wt.%) reinforcements was processed via stir casting. Optical microscope (OM) and scanning electron microscope (SEM) were utilized to study the microstructural changes. The chemical composition and phases were analyzed using energy dispersive spectroscopy (EDS) and X-ray diffraction (XRD) respectively. Evaluations were conducted on properties such as hardness, tensile strength, corrosion and wear behavior. On increasing the wt.% of TiC from 3 to 9 wt.%, it was observed that the hardness increased by 11%, the tensile strength increased by 200%, and the wear rate decreased by 50%. The composite containing 9 wt.% TiC had the lowest corrosion resistance.

Keywords: *Al 7075; TiC; stir casting; composite; corrosion; wear.*

Introduction

Aerospace, automobile, transportation, and defense industries are in dire need of a material with high specific strength, low cost and wear resistance [1-10]. Researchers emphasized the field of metal matrix composites with aluminum, magnesium and titanium as matrix materials, ceramics or organic compounds as reinforcements due to the demand for materials with enhanced properties such as high strength, hardness, fatigue resistance, environmental friendliness and lightweight. Compared to metals and alloys, aluminum matrix composites with ceramic reinforcements are renowned for their superior specific strength, hardness and modulus [11-14].

[*] Corresponding author: C. Vanitha, *vanitha@nitw.ac.in*

Aluminum 7075 is generally used due to its low density, high strength, fatigue resistance, ductility and toughness. These properties make it a perfect material for making the sheets of race car body panels. On the other hand, TiC offers high hardness, elastic modulus, low density and good wettability.

Rajnesh Tyagi et al. fabricated Al-TiC composites by in-melt reaction and compared the friction and wear characteristics of Al-TiC composites with pure aluminum. It was observed that the wear rate and coefficient of friction decreased with an increase in the weight percentage of TiC [15]. *Bhushan et al.* reported that the tensile strength and hardness of Al 7075-SiC composites increased with the increase in weight percent of silicon carbide, but tensile strength decreased when the percentage of reinforcement reached 15% [16]. *Gopalakrishnan et al.* reported that the specific strength of AA 6061-TiC composites considerably with more addition of TiC [17]. *Kalaiselvan et al.* observed that the microhardness and tensile strength of Al-B_4C composite increased with the addition of boron carbide [18]. *Sanjeev Das et al.* synthesized zircon sand/Al-4.5 wt.% Cu composite by stir casting route and noticed that the abrasive wear resistance improved with the dispersion of zircon particle in Al-4.5 wt.% Cu alloy. The abrasion resistance of the composites increased with an increase in the amount of zircon particles and decrease in particle size [19]. Limited research work has been reported on AMCs reinforced with TiC. In the present investigation, an attempt has been made to fabricate Al - TiC composites with different weight percentages of TiC (3% to 9 wt.%) and Al-7075 as matrix material.

Experimental Procedure

Materials

Al 7075 rod in hot extruded condition and TiC powder of 10 µm was used as a starting material and the chemical composition of the former is given in Table 1.

Table 1. Chemical composition of Al 7075.

Element	Zn	Mg	Cu	Si	Fe	Cr	Ti	Mn	Al
% by weight	5.24	1.89	1.20	0.38	0.21	0.20	0.09	0.056	Balance

Stir Casting

TiC powder was heated to 350°C for one hour, while the mold cavity die of the stir casting unit was preheated to 400°C to remove any moisture that may have been present. Al 7075 rod was cut into pieces, which were then placed in the crucible. At 800°C, melting was performed in a muffle furnace heated by resistance. TiC particles of 10 µm at various weight percentages (3, 6 and 9 wt.%), were added to the molten metal and stirred at a rotational speed of 300 rpm for 10 minutes to form a fine vortex and evenly disperse the TiC particles. To increase the wettability of Al and TiC, 1% magnesium was added and the molten mixture was stirred at a constant speed of 350 rpm for 10 minutes. After pouring the molten mixture through a bottom pouring arrangement into preheated molds, composites were ejected from the molds upon solidification in air.

Microstructural Characterization

Specimens cut from casted composites were polished as per the standard metallographic polishing techniques using emery papers, velvet cloth and then etched using Keller's reagent mixture (distilled water 190 ml, nitric acid 5 ml, hydrochloric acid 3 ml, hydrofluoric acid 2 ml). The etched specimens were subsequently observed under optical microscope and scanning electron microscope (SEM Make: Tescan Vega 3 LMU). The chemical composition analysis was done through SEM-EDS. The fractographic analysis of the tensile tested and wear tested samples was done using SEM to find the mode of fracture.

X-Ray Diffraction

The well-polished samples were scanned in the 2θ range of 20° to 120° with a scan speed of 0.119366°/s and step size of 0.0167113° using an X-ray diffractometer (Make: PANalytical, Model- X'pert with Cu Kα radiation (λ = 1.54056 Å) operating at 45kV and 30mA. The phases were identified from the X-ray spectrum.

Hardness Measurement

Samples were well polished and the hardness was measured using a Vickers microhardness tester (Model: HMV, G230S (E, 230V) Make: SHIMADZU) by applying a load of 0.5 kg for a dwell time of 15 seconds. At least 6 indentations were used for calculating the average hardness.

Tensile testing

Standard tensile samples were prepared according to ASTM E8 standard with a diameter of 6 mm and a gauge length of 30 mm. Tensile testing of samples was done on a Benchtop tensile testing machine (Make: HEICO) at a strain rate of 0.5 mm/min.

Wear Studies

Sliding wear tests were carried out in air at room temperature using a cylindrical pin-on-disk apparatus. During the experiment the load, sliding velocity and sliding distance were varied. A cylindrical pin of 8 mm diameter and 30 mm length was pressed on the EN31 disc. Sliding wear was determined from the change in the length of the pin using an LVDT setup. The change in length was subsequently converted to volume loss for each sample. Coefficient of friction values were obtained from the graphs using WINDUCOM software.

Corrosion Studies

Corrosion studies were carried out using an Electrochemical Work Station controlled by a computer (Model: PARSTAT 4000 Make: Princeton applied research). Potentials were measured using an Ag/AgCl reference electrode and a platinum wire as a counter electrode. All tests were performed at room temperature. The corrosion studies were conducted on both Al 7075 alloy and 7075-TiC composites with different weight percentages of TiC viz. 3%, 6% and 9% in a three electrode electrochemical cell of 500 mL capacity. The cell is made up of Pyrex glass. Tests were conducted using 3.5 % NaCl solution which is the standard corroding environment (sea water).

The electrochemical techniques used were potentiodynamic polarization measurements. Corrosion rates were calculated in terms of the corrosion current density by using Tafel curves. Potentiodynamic polarization curves were obtained by varying the applied potential with respect to the open circuit potential (OCP), from -0.25V up to +2.5V at a scan rate of 1.67 mV/sec.

Results and Discussion

Microstructural Development

Fig. 1 illustrates the SEM image of the initial TiC powder. The particles had an average particle size of 10 μm and were fine. Fig. 2 shows optical micrographs of Al 7075 alloys before and after TiC particle dispersion. Fig. 2(a) depicts the optical microstructure of the as-received Al 7075 alloy. The microstructure is made up of coarse grains, some of which were observed to be elongated. Fig. 2 (b)-(d) depicts the optical microstructures of the composite containing 3, 6, and 9 wt.% of TiC, respectively.

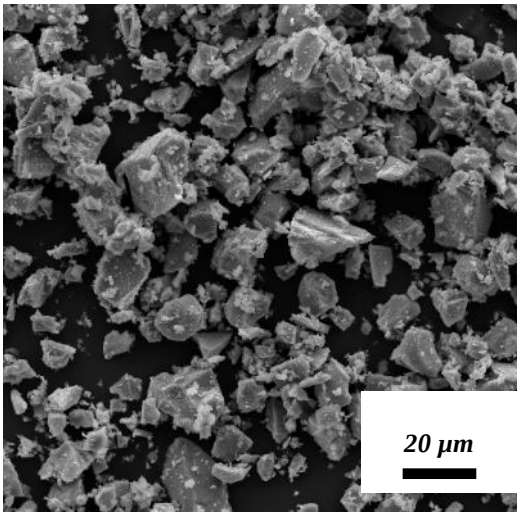

Fig. 1. SEM image of the TiC powder.

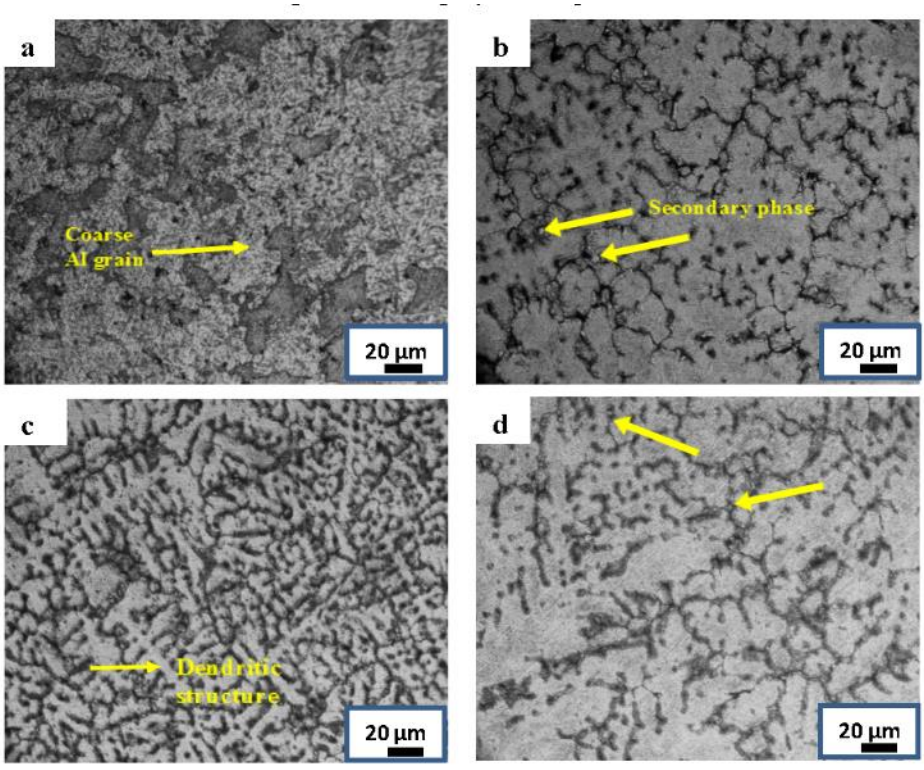

Fig. 2. Optical micrographs of the transverse plane
(a) Al7075 in the hot extruded condition (as-received); (b) Al 7075-3 wt.% TiC;
(c) Al 7075-6 wt.% TiC; (d) Al 7075-9v wt.% TiC composite.

All composites were observed to have dendritic structures with varying arm spacing. Dendrites with finer grains were observed in the composite containing 6 wt.% TiC (Fig.2(c)) and 9 wt.% (Fig.2(d)). Rapid solidification may be responsible for the formation of the dendritic structures.

Al grains demonstrated the secondary phase. Figure 3(a) depicts the SEM micrograph of Al 7075. In a condition of hot extrusion, the coarse grain was revealed.

Fig. 3(a) and Fig 3(b)-(d) show the SEM micrograph of the composite material with 3, 6 and 9 wt.% TiC particles, respectively. Non-continuous precipitates of the secondary phase were seen along the grain boundaries. Apart from these, TiC particles were also seen inside the grains and along the grain boundaries. SEM micrographs revealed the coarse grain nature of the Al 7075 in the extruded condition as shown in Fig. 3(b)-(d) the composite material showed non-continuous precipitates of the secondary.

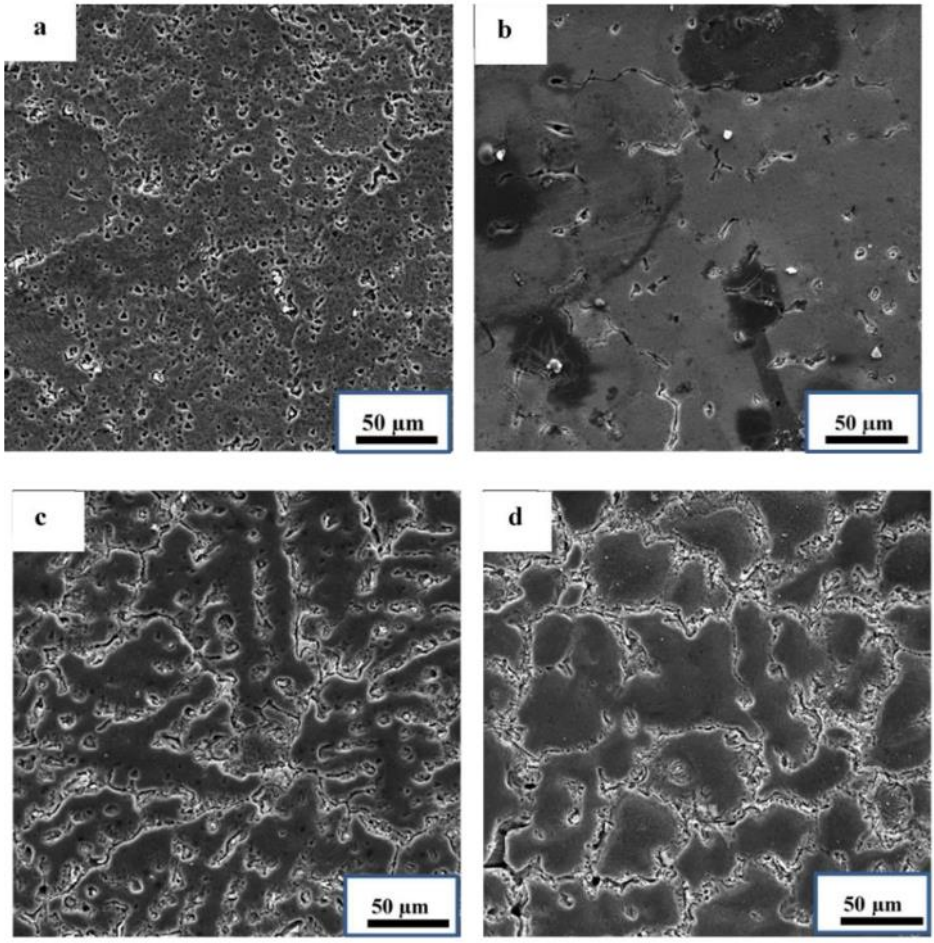

Fig. 3. SEM micrographs of Al 7075 and Al 7075 –TiC composites (a) Al 7075 Alloy (as received, hot extruded); (b) Al 7075-3 wt.% TiC; (c) Al 7075-6 wt.% TiC; (d) Al 7075-9 wt.% TiC composites.

Fig. 4(a)-(b) shows the SEM image and the corresponding EDS spectrum of the Al 7075 in the as-received or the hot extruded condition. The EDS spectrum of the Al 7075 in hot extruded alloy revealed the presence of Al, Mg, Cu and Zn. Fig. 5 (a) & (b) shows the SEM image and the elemental mapping of as received Al 7075-6 wt.% TiC. Furthermore, the EDS mapping indicated the distribution of Ti throughout the grain boundary and also the precipitates were rich in Cu and Zn.

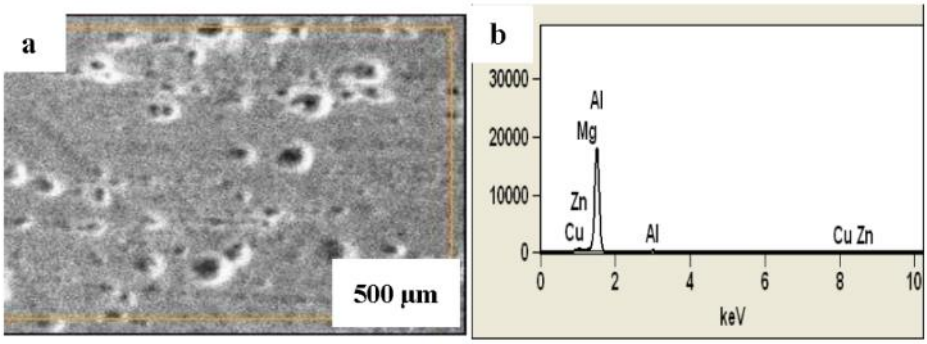

Fig. 4. Al 7075 in the hot extruded condition (a) SEM image (b) EDS spectrum.

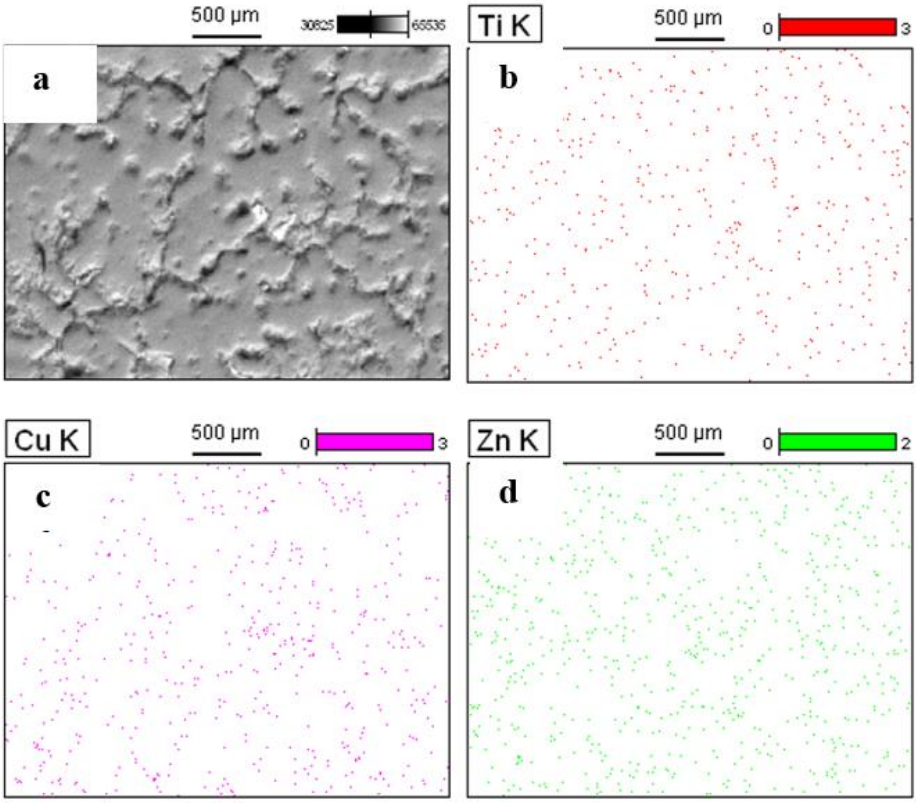

Fig. 5. Al 7075 -6 wt.% TiC alloy (a) SEM image, elemental mapping of (b) Ti, (c) Cu, and (d) Zn.

X-Ray Diffraction studies

Fig. 6. shows the XRD patterns of base metal as well as the TiC reinforced Al 7075 composites. All the composites were found to have Al_3Ti phase, this intermetallic phase may be formed due to the reaction between the base metal and TiC during stir casting. However, this phase cannot be seen in optical micrographs. Free particles of Ti and C were not detected and small peaks of TiC were detected in the composite containing 3, 6 and 9 wt.% of TiC.

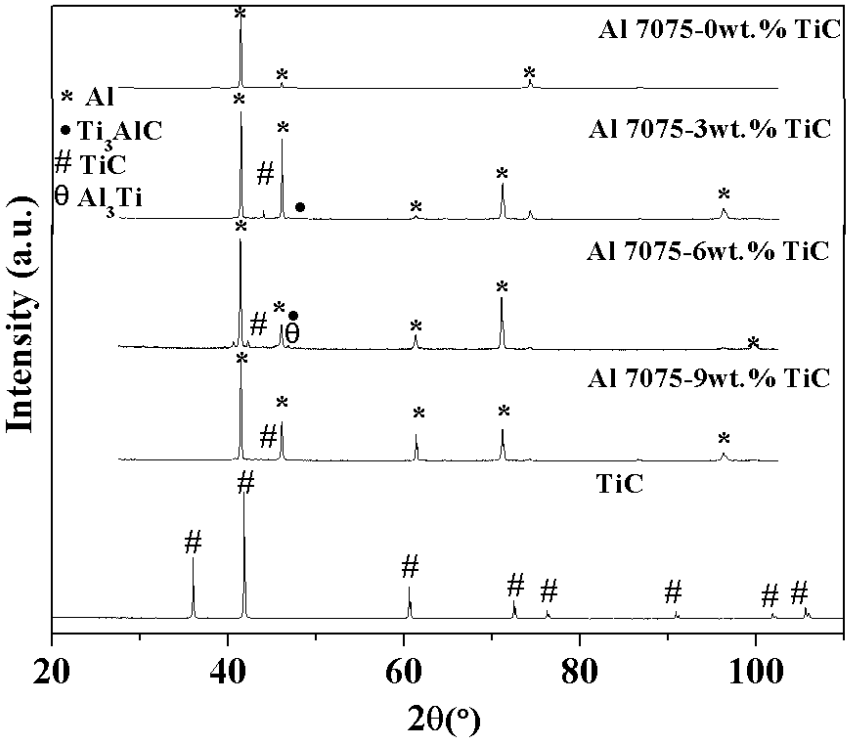

Fig. 6. XRD patterns of TiC, Al 7075 alloy and the composites with different weight percent of TiC.

Hardness

The hardness behavior of Al 7075 alloy and Al 7075/TiC composites is depicted in Fig. 7. It was observed that the hardness increased from 133 HV to 142 HV as the TiC content increased from 3 wt.% to 9 wt.%. Due to the presence of a harder TiC phase, the hardness value has increased. The XRD pattern revealed the presence of an Al_3Ti phase, which adds to the hardness improvement. Al 7075 in the hot extruded state was used as the starting material for the stir casting production of composites with varying TiC contents. As the hot extruded alloy is composed of deformed or elongated grains, it has a hardness of 187 HV. However, after melting, the resultant stir-cast 7075 alloy has a hardness of 105 HV due to its inhomogeneous or cast structure. However, compared to cast 7075 alloy, the TiC reinforced composites have a higher hardness. On increasing the

TiC content to 9 wt.% the hardness increased to 142 HV. Consequently, the composite's hardness has increased by 40 % as compared to cast 7075 alloy.

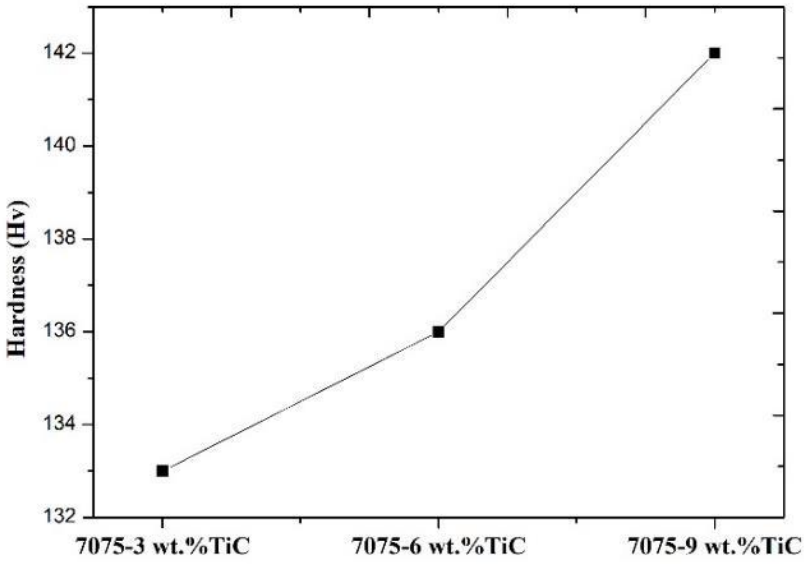

Fig. 7. Hardness behavior of composites.

Tensile properties

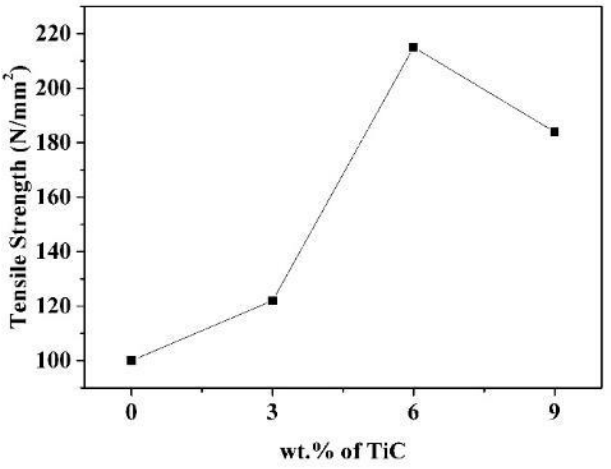

Fig. 8. Effect of TiC addition on the tensile strength of Al7075/TiC composites.

Fig. 8 depicts the tensile strength of the specimens. The specimen with the highest strength was found to contain 6 wt.% TiC. The difference in thermal expansion coefficient between the matrix and the reinforcement causes the formation of strain fields around the titanium carbide particles during the solidification of the composites. Titanium carbide

particles refine the grains of aluminum alloy, thereby increasing the surface area available for load resistance. The fairly homogeneous distribution of titanium carbide particles provides Orowan strengthening [6-8]. The clear interface and strong adhesion would delay the detachment of particles from the aluminum matrix, thereby increasing its strength.

Fig. 9 (a)-(c) depicts the SEM fractography of specimens subjected to tensile testing and reinforced with various weight percentages of TiC. In every instance, the river mark or cleavage facets indicated that the failure occurred primarily in a brittle mode. In every instance, cracks were discovered along the grain boundaries. Near the crack area, secondary phase particles were also observed, but they were not uniformly dispersed.

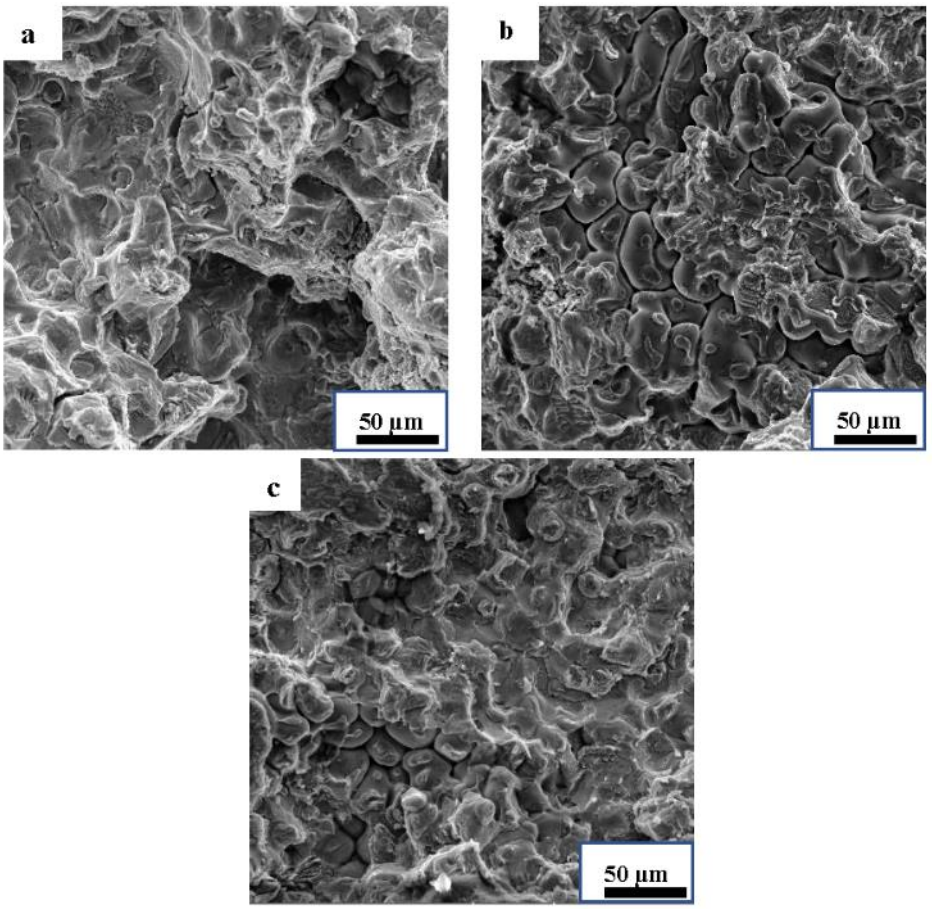

Fig. 9. (a)-(c) SEM fractography of tensile tested Al 7075 and Al 7075 –TiC composites (a) Al 7075-wt.% TiC; (b) Al 7075-wt.% TiC; (c) Al 7075-9wt.% TiC composite.

Friction and wear behavior.

Coefficient of friction (COF)

The measured values of COF were in the range of 0.2-0.378 and the lowest value of COF i.e. 0.2 was measured on Al 7075 + 9 wt.% TiC at a load of 30 N and 3.14 m/s (shown in Fig. 10). It was observed that the COF value decreased with augmented load for all the samples. The decrease in COF value may be due to the formation of oxide product at higher loads which acts as a solid lubricant [10]. The presence of small debris particles may also provide a rolling action to minimize the COF value during dry sliding.

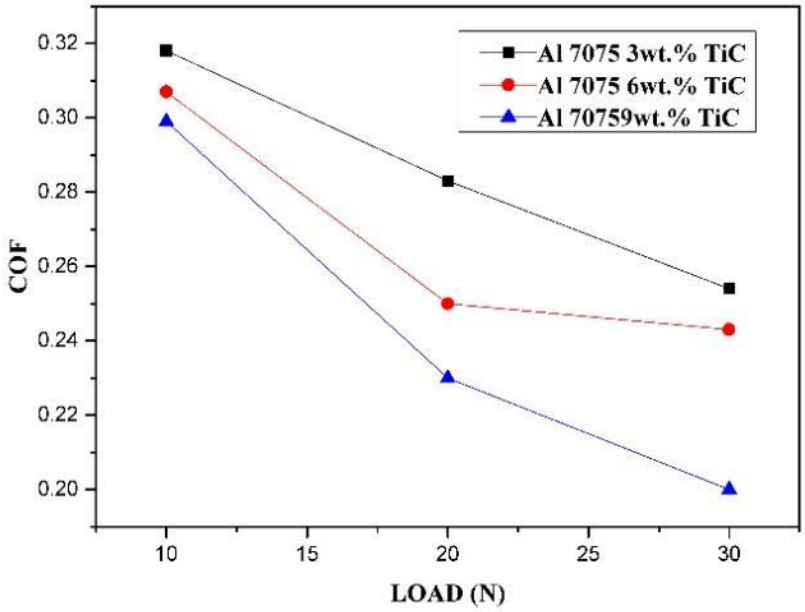

Fig. 10. Variation of coefficient of friction of Al 7075/ TiC composites with load at a constant sliding velocity of 3.14m/s.

Wear volume

Fig. 11. shows the variation of volume loss of various composites with load at a sliding velocity of 3.14 m/s. Volume loss of all the samples was measured at different loads and sliding velocities. All the samples showed continuous volume loss with time and the amount of volume loss increased with increasing load. All the samples followed similar trend. The volume loss of the composites was in the range of 1.396 to 5.15 mm^3. The wear volume increased from 3.05 to 5.15 mm^3 with increasing load from 10 to 30 N for Al 7075. + 3 wt.% TiC. In case of Al 7075 + 6 wt.% TiC and Al 7075 + 9 wt.% TiC, the calculated values of volume loss were given. The highest value of volume loss was measured on the composite containing 3 wt.% TiC. From the above data, it can be inferred that the composite with more amount of TiC was having more wear resistance [20-21].

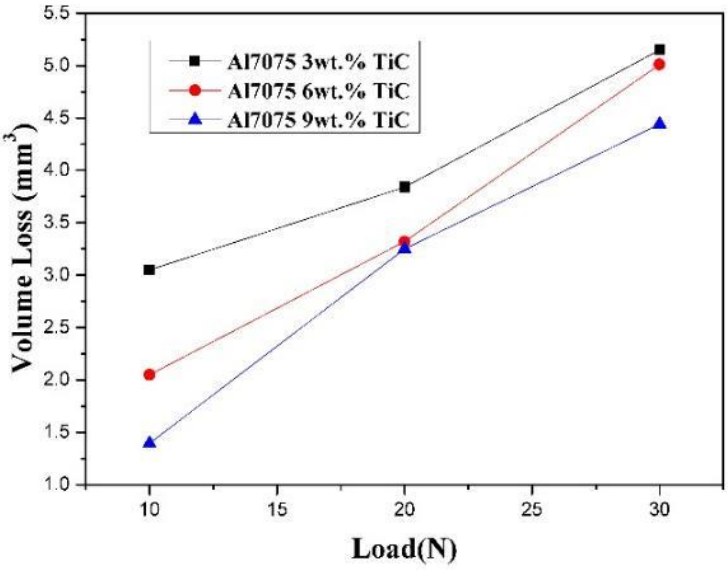

Fig. 11. Variation of wear rate with load at a sliding velocity of 3.14 m/s.

Specific wear rate

Specific wear rate was calculated for different loading conditions and different weight percentage reinforcements. It was observed that the wear rate decreased with the increase in load and decreased with the increase in the weight fraction of reinforcement [20-21]. It decreased from 10.13 to 5.15 mm^3/N-m. Al 7075 + 9 wt.% TiC was having a low wear rate of 5.1 mm^3/N-m (shown in Fig. 12).

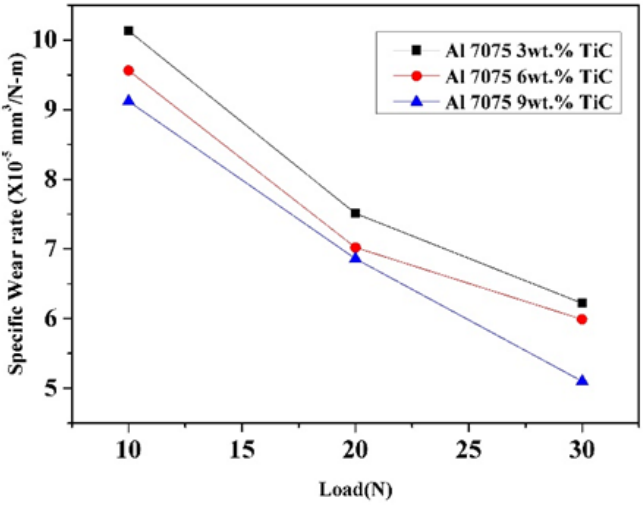

Fig. 12. Variation of wear rate with load.

Microstructural observations of worn samples

Detailed microstructural characterization was carried out on wear tested samples using SEM to understand the wear mechanism. It was observed that the composite with 3 wt.% of TiC contains coarse abrasive grooves which were reduced with increasing the amount of TiC (Fig. 13). Shallow grooves were observed on Al 7075+ 9 wt.% TiC. Fig. 14 depicts the SEM image of the oxide layer on the sample tested for wear at 30 N load. From the above results, it can be concluded that abrasive and tribo-chemical wear mechanisms predominate. The SEM image (Fig.15) illustrates the size and morphology of the wear debris produced during the wear test. Equiaxed, elongated, coarse and fine particles make up the debris. This may be a result of the cold welding that occurs during the wear test, which plays a significant role in modifying the COF value. The EDS spectrum reveals that the delamination layer is richer in oxygen than other regions (see Figure 15 (a)-(b)).

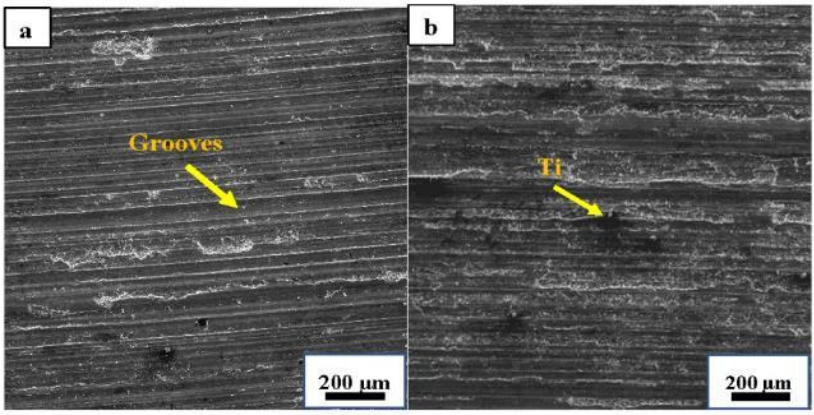

Fig. 13. SEM of the abrasive grooves. (a) Coarse abrasive grooves in Al 7075 3 wt.% TiC, (b) Shallow grooves with TiC particles in Al 7075 9wt.% TiC at 30 N load condition.

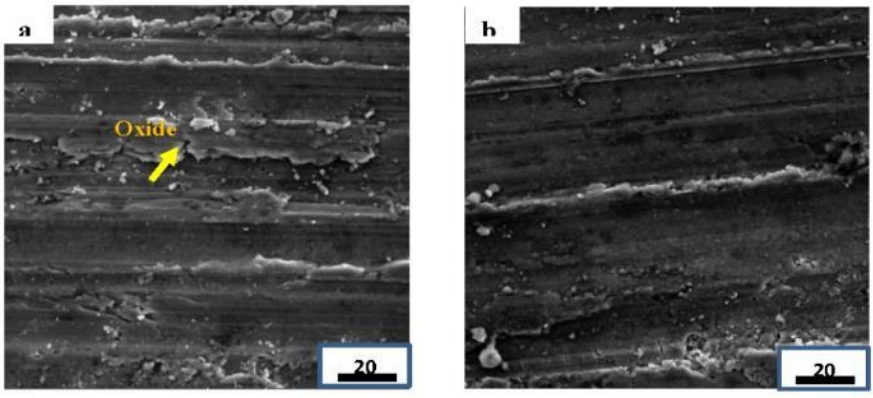

Fig 14. SEM images of the wear surface of the Al 7075 TiC based composites: (a) Al 7075- 3 wt.% TiC (b) Al 7075-9 wt.% TiC.

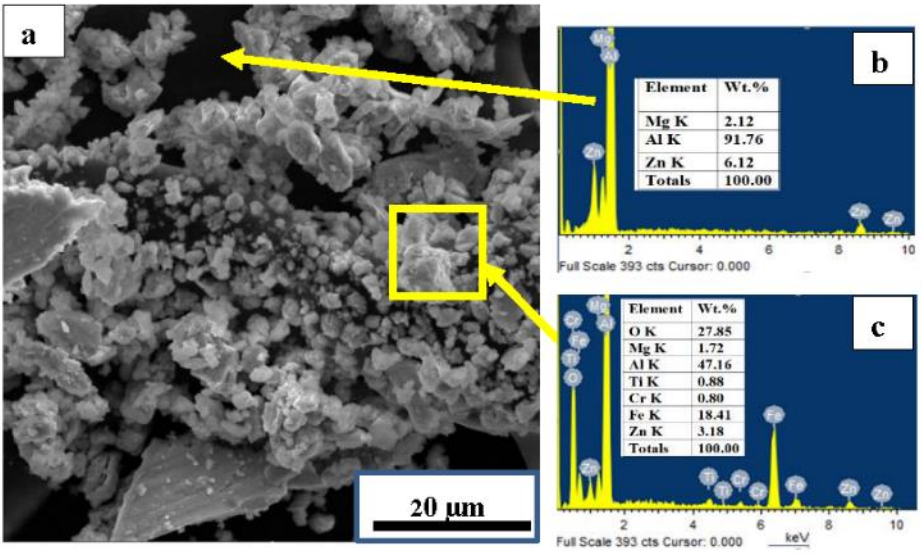

Fig. 15. SEM image and EDS spectrum of the wear debris of Al 7075/TiC composite.

Corrosion studies

Fig. 16 shows the Tafel plots of Al 7075 and Al 7075 –TiC composites tested at 3.5 wt.% NaCl solution. This clearly indicates that there is an abnormal trend from 3 to 9 wt.% TiC. Fig. 17 shows the variation of current density with different amounts of reinforcement. It was observed that the current density value was 0.61 µA/cm^2 for 3 wt.% TiC composite and increased suddenly to 4.06 µA/cm^2 for 6 wt.% TiC and then decreased to 0.33µA/cm^2 for 9 wt.%TiC (see Fig. 17). Fig. 18 shows the XRD patterns of corroded samples of Al 7075 alloy and the composites with different weight percent of TiC. It was observed that the corroded surface had the product of $Al(OH)_3$ and Al_2O_3. Fig. 19 shows the SEM images of corroded samples of Al 7075 base material (as-received) and its composites. The scanning electron micrograph of corroded samples contains the corrosion products on it. The SEM images clearly reveal the deteriorated surface of the samples. The corrosion rate in the base material is more than the composite materials. All the composites showed decreased corrosion rate except 6 wt.% with increasing the wt.% of TiC and the rate of corrosion is least in the composite having the highest percentage of TiC.

The phenomenon of a gradually decreasing corrosion rate indicates the passivation of the material due to the formation of a permanent protective layer, i.e., Al_2O_3, which plays a crucial role in the process of improving corrosion resistance [22-26]. The corrosion data revealed that the i_{corr} value decreased for 3 wt.% and 9 wt.% TiC relative to the starting material. However, for 6 wt.% TiC, the i_{corr} was the highest due to the formation of Al_3Ti, which is the result of the matrix and reinforcement during the stir casting process and subsequent solidification [22].

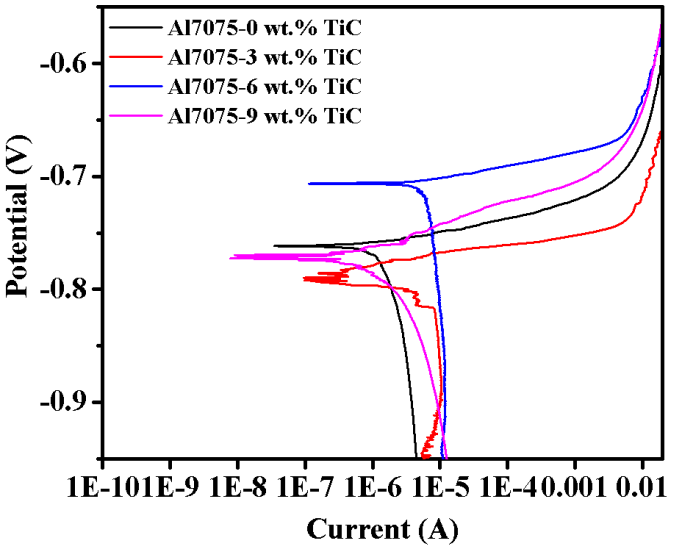

Fig. 16. Tafel plots of Al 7075 and Al 7075 –TiC composites tested in3.5 wt.% NaCl.

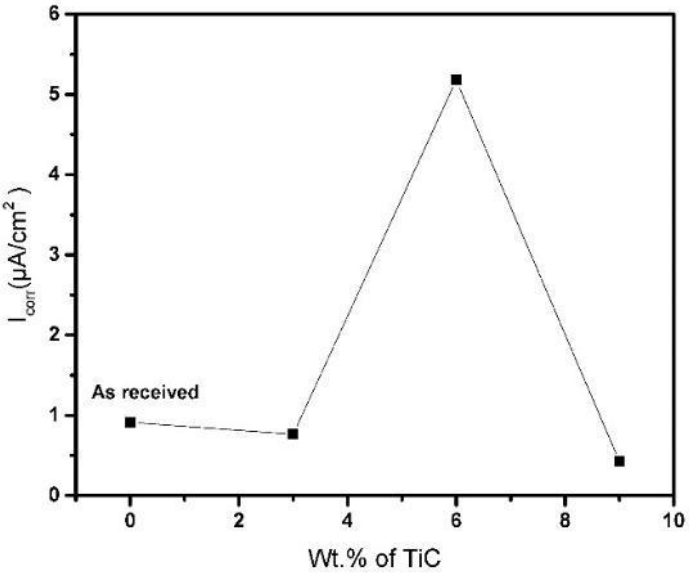

Fig. 17. Variation of current density with the wt.% of TiC in Al7075 matrix.

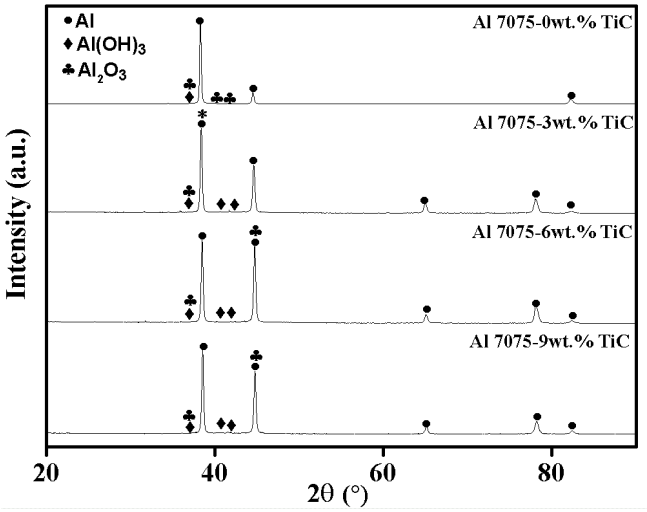

Fig. 18. XRD patterns of Corroded samples of Al 7075 alloy and the composites with different weight percent of TiC.

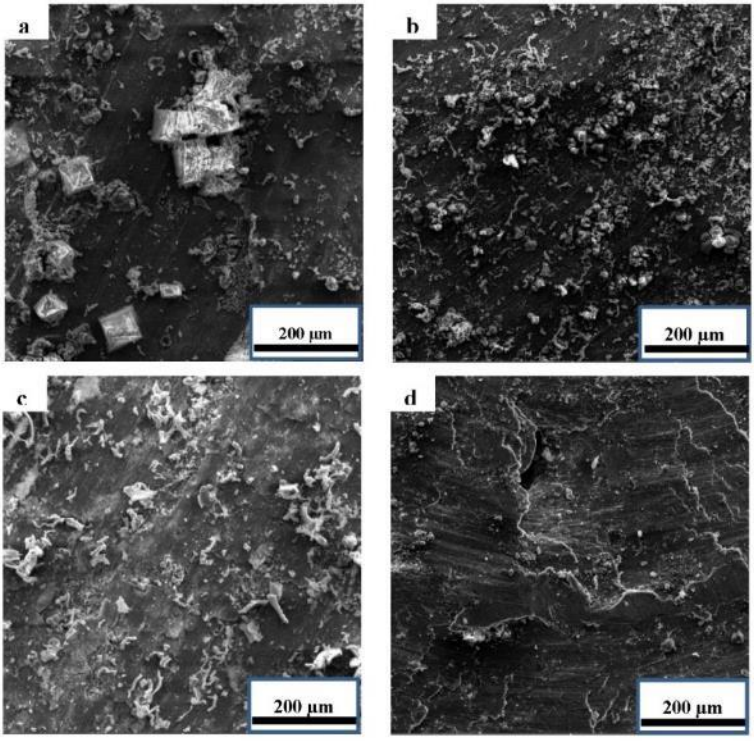

Fig. 19. SEM images of corroded samples in 3.5% NaCl. (a) Base material (as received), (b) Al 7075 + 3wt.% TiC, (c) Al 7075 + 6wt.% TiC and (d) Al 7075 + 9wt.% TiC.

Conclusions

Al 7075 TiC composites were produced by stir casting with varying weight percentages of TiC (3, 6, and 9 wt.%). Microstructure, mechanical properties and corrosion properties were evaluated. The following are the conclusions derived:

- Al 7075 TiC composites processed through the stir cast route were found to be homogeneous.
- The optical and SEM micrographs revealed the presence of secondary phase particles in the α matrix of the composite.
- XRD analysis revealed the presence of Al_3Ti in the material.
- The hardness of composites increased from 133 to 142 HV with the addition of TiC particles from 3 to 9 wt.%.
- The mode of fracture observed is mixed mode and predominantly cleavage mode.
- Wear rate and COF of all composites increased with the decrease in load and increase in the wt.% of TiC. Volume loss increased with an increase in the load.
- It was observed from the corrosion data that the i_{corr} value decreased for 3 and 9 wt.% TiC as compared to the starting material. However, for 6 wt.% TiC the i_{corr} was maximum which is due to the formation of Al_3Ti which is the resultant of the matrix and reinforcement during the stir casting process and subsequent solidification.

References

[1] S. Kumar, A. Kumar and C. Vanitha: Mate. today: proceed., 15 (2019) 21-29.
[2] S. H. Lee, J. G. Jung, S. I. Baik, D. N. Seidman, M. S. Kim, Y. K. Lee and K. Euh: Mater. Sci. Engg. A, 803 (2021) 140719.
[3] R. Zhang, W.D. Zhao, H. Zhang, W. Yang, G.X. Wang, Y. Dong, C. Ye: J. Fatigue, 153 (2021) 106463.
[4] Q. Ma, F. Shao, L. Bai, Q. Xu, X. Xie and M. Shen: Materials, 13 (2020) 4196.
[5] F. Aydin: Adv. Pow. Tech., 32 (2021) 445–463.
[6] K. Dash, S. Sukumaran and B. C. Ray: Sci. Engg. Compos. Mater., (2014) 1-19.
[7] Z. Zhang, D. L. Chen: Scrip. Mater., 54 (2006) 1321-1326.
[8] B. Al Mangour, M.S. Baek, D. Grzesiak, K.A. Lee: Mate. Sci. and Engg. A, 712 (2018) 812–818.
[9] S. Kumar, A. Kumar Mishra: Int. J. of Sci. and Res. Pub., 10 (2020) 196-204.
[10] F. Aydın: J. of Mate. Engg. and Perf., 30 (2021) 8560-8578.
[11] J. J. Moses, I. Dinaharan, S. J. Sekhar: Proceed. Mate. Sci., 5 (2014) 106–112.
[12] K. S. K. Reddy, B. R. Chitra Lekha, K.U. Sakshi, M. S. Chouhan, R. Karthikeyan, S. Aparna: Mate. today: proceed.,62 (2022) 3963-3967.
[13] Alaneme, K. Kanayo, K. O. Sanusi: Engg. Sci. and Tech., an Int. J., 18 (2015) 416-422.
[14] Md. H. Rahman, H. M. Mamun Al, Rashed: Procedia Engg., 90 (2014) 103–109.
[15] R. Tyagi: Wear, 259 (2005) 569–576.
[16] Bhushan, R. Kumar, S. Kumar: J. of Mate. Engg. and Perf., 20 (2011) 317-323.
[17] S. Gopalakrishnan, N. Murugan: Composites Part B: Engg., 43 (2012) 302-308.
[18] K. Kalaiselvan, N. Murugan, S. Parameswaran: Mate. & Des., 32 (2011) 4004-4009.

[19] D. Sanjeev, D. Siddhartha, D. Karabi: Composites Sci. and Tech., 67 (2007) 746-751
[20] M. E. Turan, F. Aydin, Y. Sun, H. Zengin, Y. Akinay: Tribology Int., 164 (2021) 107201.
[21] F. Aydin, Y. Sun: Canadian Metallurgical Quarterly, 57 (2018) 455-469.
[22] M. Shakoori Oskooie, H. Asgharzadeh, S. Sadighikia, M. Salehi: Metals, 6 (2016) 307-325.
[23] P. Rodic, I. Milosev: J. of The Electrochem. Soc., 163(2016) C85-C93.
[24] R. Bertolini, E. Simonetto, L. Pezzato, A. Fabrizi, A. Ghiotti, S. Bruschi: The Int. J. of Adv. Manu. Tech., 115 (2021) 2801–2824.